Conference Proceedings
Solar World Congress 2015
Daegu, Korea, 08 – 12 November 2015

DESIGN AND FABRICATION OF HIGHLY ENVIRONMENTAL STABLE Cr-Fe-Ni oxides/ ZrO_2-SiO_2 COMPOSITE OXIDE BASED TANDEM ABSORBER FOR SOLAR THERMAL POWER GENERATION APPLICATIONS

T. Vijayaraghavan, M. Shiva Prasad, S. Sakthivel* and S.V. Joshi

Centre for Solar Energy Materials, International Advanced Research Centre for Powder Metallurgy, and New materials, Balapur PO, Hyderabad-500 005, India.

Abstract

A new Cr-Fe-Ni oxides/ZrO_2-SiO_2 composite oxide based tandem absorber is designed and developed for high performance ORC based solar thermal applications. The Cr-Fe-Ni composite oxide based absorber layer is designed to have nanoporous structure and covered with an antireflective protective layer. The tandem absorber layer was developed by a combination of chemical and sol-gel methods. By varying process parameters like duration, temperature and withdrawal speed, different combinations of Cr-Fe-Ni oxides/ ZrO_2-SiO_2 composite absorber layers with varying refractive indices were developed on a suitable SS substrate. The optimized thickness of absorber layer along with the antireflective layer exhibited high absorptance (α= > 0.94) and low thermal emittance (ε = 0.11– 0.14 at 300 °C). More specifically, this novel tandem coating has excellent optical properties along with high corrosion resistance (withstands > 400 h in salt spray test). It has good thermal stability in an open air atmosphere and is well suited for low and medium temperature solar thermal applications.

Keywords: *Tandem absorber layer, Cr-Fe-Ni composite oxide, ZrO_2-SiO_2, antireflective layer*

Introduction

Solar collectors play an important role in areas such as hot water heating systems of buildings and steam generation for various industrial applications and power production. They convert sunlight to thermal energy which is then converted to electrical energy (Agnihotri and Gupta, 1981; Duffie and Beckman, 1991; Gordon, 2001; Kennedy, 2002; Kalogirou, 2004). Conventionally, most of the selective absorber coatings preferred for concentrated solar collector application are developed by the expensive PVD route particularly magnetron sputtering (Adsten et al.,(2000); Barshilia et al., (2008); Graf et al., (1997); Juang et al., (2010); Koželj et al., (2009); Nunes et al., (2003); Selvakumar and Barshilia, 2012; Teixeira et al., (2001, 2002); Wäckelgård et al., (2001); Yin et al., (2009); Zhang, 1998). Currently the entire concentrated solar thermal power (CSP) program is working to reduce the cost of solar thermal power technology. One of the approaches is to operate the CSP system using cost effective solar collectors in open air atmosphere conditions instead of using expensive evacuated solar collectors. To accomplish this, efficient selective collectors are needed that have high optical properties and high stability to corrosion, in addition to enhanced thermal properties. For efficient photo thermal conversion, solar collectors must have high solar absorptance (α) in an active solar region (300-2500 nm) and a low thermal emittance (ε) in the IR radiation wavelength range (3-25 μm) at an optimal operational temperature. However, most of the current coatings do not have stability against corrosion and air and this is the main problem faced while operating the collectors in an open atmosphere (Barshilia et al., (2008); Koželj et al., (2009); Selvakumar and Barshilia, 2012; Tulchinsky et al., (2014)). Moreover, the coatings need to be stable in air in case the vacuum is breached.

Selection and/or peer review under responsibility of Scientific Committee
doi:10.18086/swc.2015.04.11 Available at http://proceedings.ises.org

Solar selective coatings can have high optical properties, stability against air at operational temperature, long environmental stability, high scratch and abrasion resistance, and high mechanical integrity. Coatings prepared by an economic process (e.g. electrochemical deposition technique (Lee, 2007; Moise et al., (2001); Newby, 1999; Zeng et al., (2009)), thermal oxidation (Aries, 1986, 1987, 1991; Boydag, 1986; Douglass and Pettit, 1981), chemical oxidation (Sharma et al., (1988); Uma et al., (1987)), sol-gel process (Bostrom et al., (2008); Kozelj et al., (2009); Katumba et al., (2008)) etc on easily available substrates (e.g. stainless steel) with a combination of above mentioned properties would be a great choice for power generation by a concentrated solar power (CSP) system. Nowadays, solar absorptance of most common high-quality commercial absorbers is about 95 % and the thermal emittance is < 10 %. The techniques that have been attempted so far for the cost efficient solar absorber coatings such as electrochemical deposition, thermal oxidation, chemical and sol-gel process have faced many challenges to produce coatings with high optical efficiency, high environmental and thermal stability.

Very few studies have reported high optical efficiency with temperature and corrosion stabilities for solar absorber coatings made by sol-gel process. For example, such a coating was prepared from polysiloxane as a binder and Co_3O_4 as a spinel pigment on 304 stainless steel by spin-coating (Andrea Ambrosini et al., (2010)). Spectrally selective absorber coatings were prepared by spin- coating of nickel nanoparticles embedded in alumina and coated with an antireflective layer made of silica, alumina, or silica–titania mixture (Bostrom et al., (2005)); Orelet al., (2003)) reported doping of $CuCoMnO_x$ by Ti in a polysiloxane resin. The films were used in order to increase the weather resistance and showed absorptance of 0.86 – 0.91 and emittance below 0.036. Tulchinsky et al., (2014) reported the thermal chemical reaction between a titania sol–gel precursor with the copper manganese spinel to form a new material, $Cu_{0.44}$ $Ti_{0.44}$ $Mn_{0.84}Fe_{0.28}O_3$, having a bixbyite structure. Although solar absorptance of the films was reported around 97.4 %, no data was provided for the emittance of the film. Chao-Ching Chang reported poly(urethane)-based solar absorber coatings containing copper chloride and nanogold composite synthesised by solution-chemical technique. The solar absorptance and thermal emittance of this coating were shown to be only around 0.846 and 0.09, respectively (Chao-Ching Chang et al., (2013)). Copper–cobalt oxide thin films deposited on aluminium substrates via a facile sol–gel dip-coating method showed solar absorptance of 3.4 %. (Amun Amri et al., (2013)). A higher value of solar absorptance and better stability is needed for the films to be suitable for concentrated solar thermal power application.

Martin Joly et al., (2013) produced multilayered chrome-free black selective surfaces for solar thermal energy conversion by a low-cost sol–gel dip-coating method. The optical properties of solar absorptance and thermal emissivity at 100 °C of the Cu–Co–Mn–Si–O based nano crystalline thin films were shown around 0.95 and 0.12. The coatings were stable up to a maximum of 360 °C in air which surpasses that of the conventional robust black chrome coatings existing in the market. But there was no report on the weather stability of the novel multilayer absorber coating.

For concentrated solar thermal power plant (CSP) application, coatings are required in a large area and development of solar receiver tubes with all the properties like high solar absorptance, low thermal emissivity, high weather and thermal stabilities by an economic way is the main objective in order to reduce the cost of solar electricity production. In view of the above, herein, we report a novel Cr-Fe-Ni oxides/ ZrO_2-SiO_2 nanocomposite oxide based tandem absorber system developed by a combination of chemical oxidation and sol-gel process for high performance ORC based solar thermal applications having excellent optical properties along with high corrosion resistance and good thermal stability in an open air atmosphere and their optical and structural characterisations.

2. Experimental

2.1. Sample preparation

The thin nanoporous structure composite oxides of absorbing layers were developed on smooth highly specular reflecting mirror of stainless steel substrates. The base absorber films were developed by controlled chemical oxidation process on a special variety of stainless steel tube (SS-316) having the composition of C: 0.08, Mn: 2, P: 0.045, S: 0.030, Si: 0.75, Cr: 16-18 and Ni: 10-14**;** and Fe: 69-73 wt % respectively, using a precise temperature controllable chemical bath reactor and an optimum parameters like molar ratio of acid mixture, temperature, and duration. 1M sodium dichromate salt dispersed in a mixture of sulphuric acid and water (3:5) was used for the development of nanoporous base absorber layer. The detailed preparation procedure of the absorber layer has been described elsewhere (Sakthivel et al., (2013)). In a preliminary step of the process, the SS tube sample is cleaned with a mild detergent solution and rinsed with tap water followed by deionised water and finally wiped with a soft cotton cloth using an organic solvent, preferably

isopropyl alcohol (IPA), to make it free of any external impurities adhering to the surface. The cleaned substrate is then dried either by an air drier or by keeping it at 100 ^{0}C for 5-10 min in an air–oven. The dimensions of SS tube used for this study were 500 mm x 500 mm x 1.25 mm (L x W x Thickness).

2.2. Development of nanoporous composite absorber layer on SS 316 tubes

The cleaned substrates are immersed into an acid bath for chemical oxidation in a temperature range of 80-90 °C for 20-30 min. During the chemical oxidation process, the metal atoms on the surface of substrates are partially oxidized by the acid mixture to obtain a type of nanoporous composite oxide layer. After chemical oxidation, the SS tubes turned to grey in colour with a glassy appearance. The absorber layer developed SS tube was then washed thoroughly with tap and distilled water and finally wiped with a soft cotton cloth using with an organic solvent, preferably isopropyl alcohol (IPA). The cleaned absorber layer developed substrate was then dried by an air drier for 2-5 min.

2.3. Development of optical enhancing layer on absorber layer coated SS 316 tubes

After drying, the optical enhancing protective layer comprising ZrO_2–SiO_2 composite, was deposited by dip coating process using a composite sol obtained by mixing zirconium propoxide and 3-glycidoxy propyltrimethoxysilane (GPTS) compound in a mixture of isopropyl alcohol (IPA, Alfa Aesar) and Isopropoxyethanol (IPE, Alfa Aesar) to obtain a stable suspension. The composition of the coating suspension for this layer was in the ratio of Zr (n-Pro): IPA: IPE: GPTS = 6.94:78.52:12.94:1.60 (wt %). ZrO_2-SiO_2 composite coating sol was coated on the absorber coated steel substrates using dip-coating technique. No binder/additive was used for the coating. Increase in withdrawal speed resulted in increase of coating thickness and in turn the packing density. To obtain highly optical enhancing thin films, the coating speed and curing temperature were altered from 2 mm sec^{-1} to 5 mm $^{-1}$sec and 100-300 °C respectively. It was noted that the film showed a high optical enhancing (antireflection) property (> 8 % solar absorptance from 300-2500 nm) even at low possible curing temperature, 100 °C. Hence it is suitable for making cost effective tandem absorber layer for solar thermal application.

2.4. Characterization methods

Optical and structural properties of the absorber layers were measured after the coating layer development. The diffuse reflection spectral measurements in the UV/ Vis /near-IR region were carried out by a Cary 5000 spectrophotometer equipped with a standard integrating sphere (110 mm dia) at room temperature in the spectral interval of 0.3 – 2.5 μm with a scanning speed of 1200 nm min^{-1}. Normal emittance measurements in the infrared wavelength region were carried out by a Bruker vertex 70 FTIR (Fourier Transform Infrared) spectrophotometer equipped with a standard integrating sphere using an evaporated gold mirror as a reference plate. All the measurements were done in the spectral interval of 2.5 – 25 μm with a scanning velocity of 2.5 KHz.

The normal absorptance (α) and emittance (ε) values were calculated using standard equations as described in literature (Bostrom et al., (2003)). The solar absorptance, α_{sol} of the sample was calculated as a weighted fraction between absorbed radiation and incoming solar radiation using an AM 1.5 spectrum. The direct normal solar irradiance, I, is defined according to the ISO standard 9845-1 (1992) where an air mass of 1.5 is used (Bostrom et al., (2003)).

The thermal emissivity (thermal loss) of coatings corresponding to a particular temperature (ε_t) was calculated as described in literature (Sakthivel and Srinivasa rao, 2015). However, values of thermal emittance of black body at each temperature were used instead of using a theoretical black body distribution as is generally used in literature (Bostrom et al., (2003); Lundh et al., (2010)). FTIR spectrometer equipped with the standard accessories of black body furnace and a high pressure cell (sample compartment) supplied by Bruker optic GmbH was used for the measurement of thermal radiation emittance. For thermal emissivity calculation, initially the thermal radiation emittance spectra (2.5-25 μm) of both black body and selective absorber layer coated sample were measured one after another by heating black body furnace and coated sample in the sample compartment at temperature range starting from 100 to 300 °C. Finally, the thermal emissivity was calculated by using this formula, ε_t= sample emittance radiation /Black body emittance radiation generated at the same temperature from 2.5-25 μm.

X-ray diffraction pattern was recorded by using Bruker AX D8 XRD equipment having CuK_α X-ray source. The scan was taken in the range 0-100° with an increase of 0.01°at duration of 2s step^{-1}. Surface morphology of absorber layers was studied by field emission scanning electron microscopy, FESEM (Hitachi model S4300SE/N) operated at 20 kV. Energy dispersive spectroscopy (EDS) was carried out for all the films during SEM study.

Coating thickness and refractive index of the composite layers were measured using a spectroscopic ellipsometer (Model: M-2000V, J. A. Woollam Co. Inc.) in the wavelength range of 350–1000 nm. Water contact angle was measured by a drop shape analyser DSA 100 (Kruss GmbH, Germany) to verify the surface roughness (hydrophobicity/hydrophilicity) of the absorber layer. The chemical composition and oxidation state of the composite layers were analysed by X-ray photoelectron spectrometer (Omicron-ESCA+) equipped with Al Kα anode and Raman spectrophotometer (Model: HR 800, Horiba Jobin-Yvon, France).

3. Results and discussion

3. 1. Design of Cr-Fe-Ni nanocomposite oxide / ZrO_2-SiO_2 tandem absorber

The schematic diagram of Cr-Fe-Ni nanocomposite oxide / ZrO_2-SiO_2 tandem absorber is shown in Fig. 1. An absorber–reflector tandem absorber concept was used to develop the absorber on SS substrates, where in the Cr-Fe-Ni nanocomposite oxide layer and smooth SS surface (surface roughness around <1 micron) act as absorber layer and infrared reflector, respectively. It is well known that the optical properties of transition metal based coatings can be tailored by controlling the stoichiometry, which affects the density of free electrons in the d band (Seraphin, 1979). Based on this concept, the first absorber layer Cr-Fe-Ni composite oxide was designed to have higher amount of Cr oxide content (called as HfMoN(H)) than the Fe and Ni oxides in order to achieve high selective property with suitable refractive index which matches with second layer (optical enhancing layer (antireflective layer)) for further optical enhancement.

The tandem design used for the fabrication of highly environmentally stable absorber system is illustrated in Fig. 1. Cr-Fe-Ni nanocomposite oxide layer with nanoporous structure (11-14 nm pore size) was prepared by controlled chemical oxidation process using optimum process parameters like a process temperature, 80-90 ^{0}C, process duration, 20-30 min and an optimum concentration of acid mixture, 1M sodium dichromate salt dispersed in a mixture of sulphuric acid and water (3:5), respectively. Followed by the deposition of absorber layer by the above described controlled chemical oxidation, the optical enhancing layer (antireflective layer) with weather resistant property is deposited by the dip coating process using a composite sol of ZrO_2-SiO_2 prepared by a sol-gel method.

Figure 1. Schematic diagram of the Cr-Fe-Ni oxides / ZrO_2-SiO_2 composite oxide layer deposited on stainless steel tube

3.2 .FE-SEM

The FE-SEM representative images of Cr-Fe-Ni nanocomposite oxide absorber layer developed on SS-316 mirror (smooth surface) are shown in Fig. 2. It can be observed in this figure that the surface morphology of Cr-Fe-Ni composite oxide absorber layer on SS-316 polished surface (Fig. 2a) comprises a nanoporous morphological structure of 13–17 nm in diameter, because of the controlled chemical oxidation of metal atoms on the surface of SS plate. Particularly, Cr, Fe and Ni were the predominant metal atoms involved in the oxidation process. The surface morphology of ZrO_2-SiO_2 (Fig. 2b) deposited on the absorber layer in the tandem system uniformly covered all the nanopores. Furthermore, the layer deposited on the absorber layer for the optical enhancement and protection from weather and corrosion was very uniform and without cracks and pinholes.

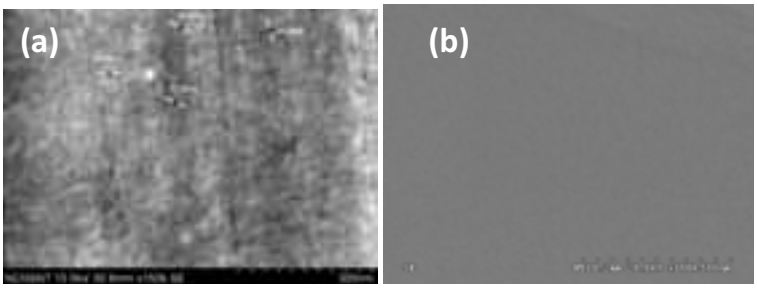

Figure 2. FE-SEM surface morphology of (a) Cr-Mn-Fe composite absorber layer with nanoporous structure (Pore size around 13-17nm); (b) Tandem absorber layer of Cr-Fe-Ni oxides / ZrO_2-SiO_2 composite oxide layer generated on SS tube

3.3. X-Ray Diffraction (XRD) results

The results of the incident angle XRD studies for the absorber layer comprised of Cr-Fe-Ni composite oxide layer developed using optimized conditions are shown in Fig. 2 and are compared with the diffraction peaks of bare SS-316 sample. The peaks observed in the bare substrate indicate an austenitic type of steel (Fig. 3 FCC peaks labelled "a"). It is surprisingly noted that the XRD patterns of chemically oxidized samples are quiet similar to the bare substrate. The reason could be that a high content of iron (69-73 %) in the substrate which dominated during analysis as compared to other components like chromium, manganese, nickel which are presented in lower concentration. Moreover, the atomic number of chromium, nickel, and copper are very close to metallic iron. From XRD analysis it is quite difficult to distinguish if the element is in low concentration or the layer thickness in nano range.

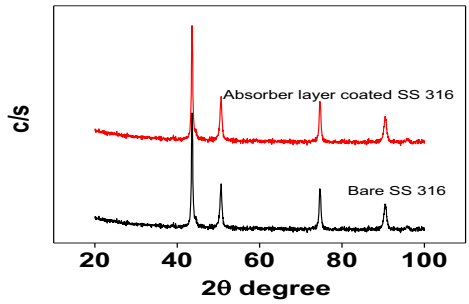

Figure 3. XRD patterns of both bare and absorber layer developed on SS-316 polished plate

3.4. X-Ray photoelectron spectroscopy (XPS) results

The coating compositions of the base absorber layer and the oxidation states of each element were clearly confirmed by XPS. Fig. 4 (a-d) shows the high resolution core level X-ray photoelectron spectra (XPS) for an absorber layer developed on SS 316 polished surface. The Cr 2p spectrum (Fig. 3(a)) consists of 2 peaks centered at 576.73 and586.35, which originate from Cr $2p^{3/2}$ and Cr $2p^{1/2}$ electrons in Cr_2O_3 (Hsin-Yen Cheng et al., (2013); Teixeira et al., (2002); Wu et al., (2013)). The Fe 2p spectrum (Fig. 3(b)) exhibited four peaks centered at 707.14, 709.29eV, 726.40 and 730.03 which correspond to Fe $2p^{3/2}$ and Fe $2p^{1/2}$ of FeO and Fe_2O_3 (Srinivasa Rao and S.Sakthivel, (2015); Tulchinsky et al., (2014)). The Ni 2p spectrum (Fig. 3(b)) exhibited 2 peaks centered at 853.05 and 870.39 eV, which correspond to Ni $2p^{2/3}$ and Ni $2p^{1/2}$ of NiO (Ewa Wackelgard et al., (1998)). The 1s spectrum of oxygen (Fig. 3(d)) of the absorber coating (Cr-Fe-Ni oxide layer) revealed the presence of two peaks centered at 530.42 and 531.25 eV, which correspond to oxides Fe, Ni and Cr. From this result, it is clear that the nature of composite absorber layers formed by the controlled chemical oxidation method may depend upon the process conditions. According to XPS analysis, the surface composition of the absorber layers in atomic percentage was in the ratio of 17.97: 6.28: 2.22: 73.53 (Cr: Fe: Ni: O).

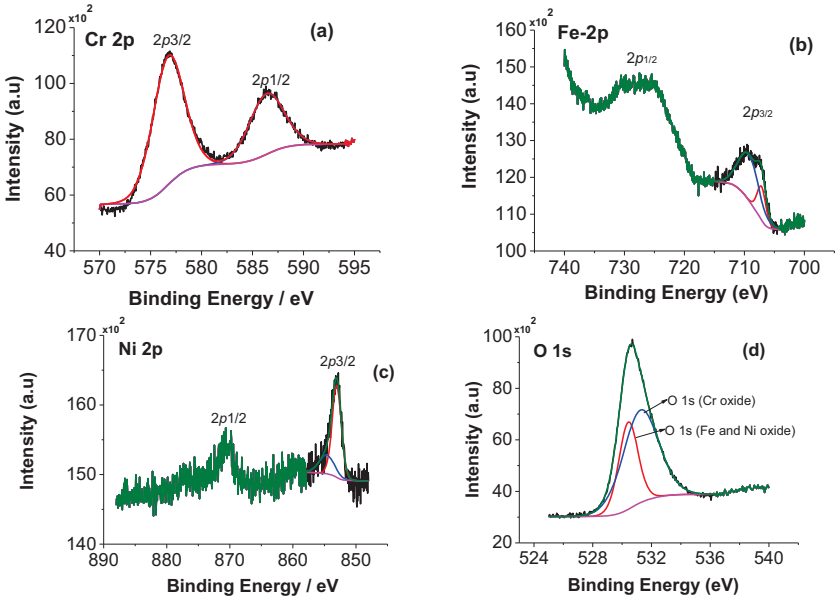

Figure 4. X-ray photon electron spectra of absorber layer developed on SS 316 polished surface

3.5. Solar absorptance of single and tandem absorber systems:

Fig. 5 and Table. 1 summarize the reflectance spectra measurement at room temperature for the absorptance characteristics of the corresponding nanocomposite selective absorber layer with nanoporous morphological structure prepared with the optimum conditions of process temperature, duration, and using with an optimum concentration of acid mixture: 85 °C, 20 min and 1M sodium dichromate salt dispersed in a mixture of sulphuric acid and water (3:5), respectively. The reflectance spectrum of Cr-Fe-Ni nanocomposite oxide layer with nanoporous morphological structure shows a little higher reflectance in the solar range corresponding to a low solar absorptance of 86.1 %. However, the absorber layer further coated with the optical enhancing layer (antireflective layer) using a composite sol of ZrO_2-SiO_2 by sol-gel dip coating process. The optical enhancing layer deposited with an optical withdrawal speed of 3 mm sec^{-1} followed by curing at 300 °C for 2 h exhibits high solar absorptance, 94.3 %.

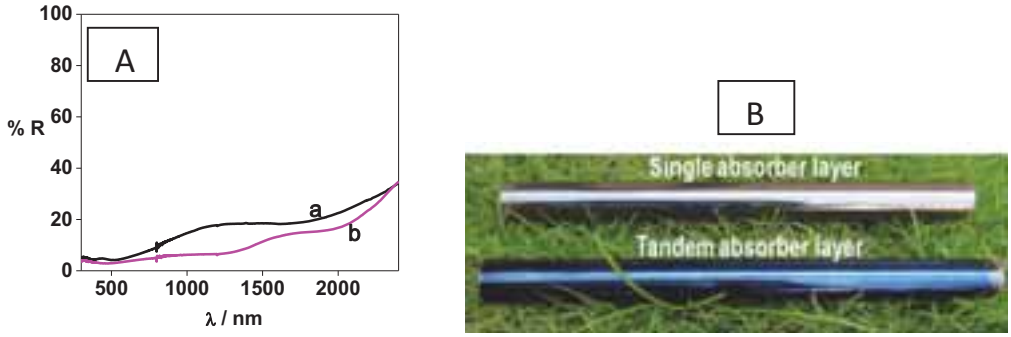

Figure 5A. Comparison of reflectance spectra of Cr-Fe-Ni nanocomposite oxide (a) and Cr-Fe-Ni oxides /ZrO_2-SiO_2 Tandem absorber layers (b), 5B. Image of 0.5 m long single and Tandem absorber layers coated SS 316 tubes.

3.6. Thermal emissivity characterization:

Thermal emissivity characterisation of the both single absorber layer (Cr-Fe-Ni nanocomposite oxide layer) and two layer tandem absorber layer (Cr-Fe-Ni nanocomposite oxide layer/ ZrO_2-SiO_2 sol-gel layer) exhibits high solar absorptance developed on the polished surface of SS 316 and was carried out by FT-IR spectrophotometer using special accessories like a black body furnace and high temperature sample cell unit. The thermal emittance of both black body furnace and samples were measured at different temperatures starting from 100 °C to 300 °C with an interval of 50 °C. Finally, the thermal emissivity of the coatings was

calculated from the measured thermal emittance data of sample and black body furnace using the standard equation as described in the literatures (Carlsson et al. (2000), Öhl et al. (2004), Price et al. (2004)).

Typical thermal emissivity spectra were derived for single and tandem absorber layers from their emittance and black body emittance spectra were recorded at different temperatures from 100-300 °C and represented in Fig. 6 and Table. 2. The thermal emissivity of heat radiations from both types of layers on SS substrates are increased with increasing of temperature. Compared to the single absorber layer coated sample, a little lower value of emissivity is noted for the tandem absorber sample due to covering of nanopores in the absorber layer by the AR layer. Further, it is clearly noted that the tandem absorber layer shows low thermal emissivity value of 0.067-0.144 at 300 °C. However, the single nanocomposite absorber layer having nanoporous morphological structure shows a high thermal emissivity range of 0.106-0.172 measured from 100 °C to 300 °C. The reason for observing a high thermal emissivity could be the presence of pores in the absorber layer.

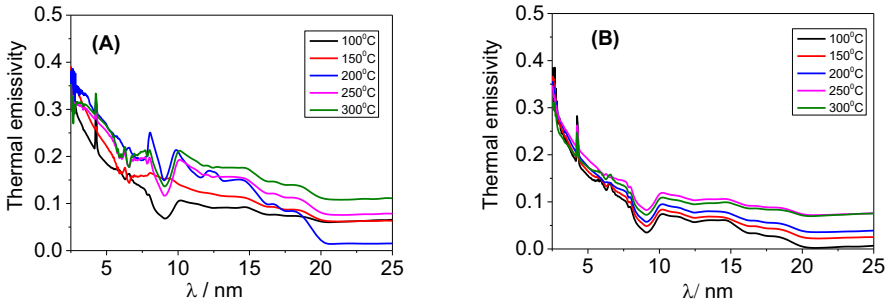

Figure 6. (A) Thermal emissivity spectra of single absorber layer (Cr-Fe-Ni nanocomposite oxide layer) and (B) Two layer tandem absorber layer (Cr-Fe-Ni nanocomposite oxide layer/ ZrO_2-SiO_2 sol-gel layer) developed on SS-316 polished surface measured at different temperatures.

Table 1. Thermal emissivity data of single absorber layer (Cr-Fe-Ni nanocomposite oxide layer) and two layer tandem absorber layer (Cr-Fe-Ni nanocomposite oxide layer/ ZrO_2-SiO_2 sol-gel layer) measured at different temperatures.

Temperature (^{0}C)	ε (2.5-25μm)	
	Single	Tandem
100	0.106	0.067
150	0.127	0.079
200	0.138	0.090
250	0.150	0.116
300	0.172	0.144

3.7. Optical thickness and refractive index results of nanocomposite oxide absorber and optical enhancing layers

The thickness and refractive index of Cr-Fe-Ni nanocomposite absorber and ZrO_2-SiO_2 based optical enhancing layer (antireflective along with corrosion protection) developed by the optimum conditions were estimated by ellipsometer are represented in Table. 2. The experimental data has been fitted with theoretically simulated spectra using a suitable mathematical model for optical constants of the materials. From the fitting, the thicknesses of the layers and the optical constants of the materials have been determined similar as our earlier work (Sakthivel and Srinivasa rao, 2015). The deposited absorber layer (Cr-Fe-Ni nanocomposite oxides) and optical enhancing layer (ZrO_2-SiO_2) layers were modelled using the Cauchy dispersion model for generating the refractive indices and extinction coefficients spectra. The thickness and refractive index values of the absorber layer are around 140 ± 5nm and 1.88 ± 0.01and optical enhancing layer 70 ± 5nm and 1.70 ± 0.01, respectively. High optical properties of high solar absorptance, >94 ±0.1% and low emittance,

<0.15±0.01 were observed only for the optimum thickness of the absorber and optical enhancing layer. The absorber layers generated at the thickness of < or > 140 ± 5 nm with optical enhancing layer (ZrO_2-SiO_2) at the thickness of 70 ± 5 nm the optical properties of either absorptance or emittance were not observed in a satisfactory level. Moreover, the thickness of the absorber layer was found to increase from 140 ± 5nm to 300 nm with increase in the net deposited oxide content on the substrate due to increase of process duration from 20 to 30 min. The refractive index value was also found to increase from 1.88 to 2.41 due to increase of oxide content.

Table 2. Summarises the optical property, thickness and refractive index data of composite oxide and Tandem absorber layers

Sample	α	$\varepsilon_{300\,^0C}$	Thickness (nm)	Refractive index
Cr-Fe-Mn composite absorber layer	86.28	0.172	140	1.88
Cr-Fe-Mn /ZrO_2 -SiO_2 Tandem absorber layer	94.30	0.144	140/70	1.88/1.7

3.8. Corrosion stability of nanocomposite oxide absorber layer and Tandem absorber system

To understand the corrosion and thermal resistance behaviour of both single and tandem absorber system, the coatings were subjected to a salt pray test for proving the corrosion and weather stability in a salt pray chamber following the *ASTM method (ASTM 13117)* using 5 % NaCl solution and generating vapours at a temperature of 35 °C /min. After every cycle test (24 hours) the coating was inspected for the change in properties of solar absorptance and thermal emissivity at a maximum temperature, 300 °C by UV-Vis-NIR and FT-IR spectrophotometer with thermal emissivity accessories of high pressure cell and black body furnace. According to the salt spray experiments, the tandem absorber layer was found to have no changes in its absorptance and emittance properties even after 20 days salt spray test. However, the sample deposited with the nanocomposite layer only could withstand the salt spray test for a maximum of 10 days.

Table. 3: Changes of solar absorptance and thermal emittance measured at 300^{0}C of single and Tandem absorber system developed on SS-316 polished surface.

Duration (day)	Abs (α)		ε_{300^0C}	
	Single	Tandem	Single	Tandem
	86.21	94.41	0.172	0.146
1	86.13	94.29	0.173	0.143
2	86.91	94.37	0.172	0.146
5	86.03	94.22	0.175	0.141
10	86.13	94.30	0.176	0.144
15	84.16	94.35	0.220	0.143
20	81.57	94.19	0.231	0.145

3.9. Thermal stability

An important requirement for absorber coatings is long-term thermal stability, ideally in air. Thermal stability is sometimes based on thermal properties of the individual materials or the processing temperature parameters. Since thermal instabilities and degradation of the solar absorber layers are major parameters of interest for long-term stability of the selective solar absorbers, the stability of the single and tandem absorber layer developed on the polished surface (SS 316) was tested under a thermal cycle test (maximum up to 300 °C) suitable for medium ORC based solar collectors usually operating at the temperature range from 200 °C-250 °C. To determine the durability and thermal stability of the coatings a precise temperature controllable furnace (Nabertherm model L 5/12/P330**)** in an open air environment and was utilized for this

study. It has digital PID-temperature control and temperature programme with 40 segments to allow the operator to run the furnace with a specific heating rate, soaking and cooling hours. To evaluate the thermal stability, the samples were annealed in air at 300 °C and for a maximum of 100 cycles. Each cycle comprised of 2h heating to attain 300 °C, 2h soaking duration, and 5-6h cooling to reach the ambient temperature. The dependence of optical properties of the coatings on the thermal treatment was investigated. The solar absorptance and thermal emittance at 300 ^{0}C were measured using a UV–Vis–IR and FT-IR-Spectrophotometer and the detailed measurement procedures have been reported elsewhere [Sakthivel et al]. According to the experiments, both the single and tandem absorber layer was found to have no remarkable changes in their absorptance and emittance properties even after 100 cycles. However, after 350 °C the coatings started to degrade, >10 % of absorptance changes were observed even after 10 cycles and no changes in thermal emissivity property.

Table 4. The effect of annealing at 300 ^{0}C in air, on the solar absorptance and thermal emittance measured at 300 ^{0}C single and Tandem absorber system developed on SS-316 polished surface.

Cycle	α_{sol}		$\varepsilon_{300^\circ C}$	
	Single	Tandem	Single	Tandem
0	86.29	94.32	0.170	0.143
10	86.32	94.56	0.172	0.144
20	86.41	94.18	0.171	0.145
30	86.24	94.53	0.169	0.141
40	86.46	94.48	0.172	0.144
50	86.42	94.41	0.173	0.145
60	86.35	94.49	0.175	0.144
70	86.26	94.43	0.173	0.145
80	86.31	94.22	0.171	0.146
90	86.25	94.37	0.173	0.142
100	86.23	94.35	0.174	0.146

4. Conclusion

A novel tandem layer design of Cr-Fe-Ni oxides/ZrO_2-SiO_2 composite oxide selective absorber layer developed on an austenitic stainless steel (SS-321) substrate has proved to show have excellent optical properties (α_{sol}:94.3 %; $\varepsilon_{300\,^\circ C}$; 0.144) along with high corrosion resistance (>400 h withstand in salt spray test) and good thermal stability in an open air atmosphere. This novel design will thus allow an increase in the operating temperature in the solar field up to 300 ^{o}C, leading to improved performance and reduced cost of ORC based solar thermal power generation.

Acknowledgements

The authors are grateful to Dr. G. Sundararajan, Director of ARCI for his great support for this research. They also wish to thank Mr. A. Srinivasa Rao, Mr. V. Premkumar and Dr. H. Neha for their help during deposition experiments and characterizations.

References

Agnihotri, O.P., and Gupta, B. K., 1981. Solar Selective Surfaces. 1st ed. Wiley-Interscience Publication, New York.

Amun Amri, XiaoFei Duan, Chun-Yang Yin, Zhong-Tao Jiang, M. Mahbubur Rahman, Solar absorptance of copper–cobalt oxide thin film coatings with nano-size, grain-like morphology: Optimization and synchrotron radiation XPS studies, Applied Surface Science 275 (2013) 127– 135.

A. Srinivasa Rao and S. Sakthivel, A highly thermally stable Mn-Cu-Fe composite oxide based solar selective absorber layer with low thermal loss at high temperature, Alloys and compounds. 644 (2015) 906-9151.

B. O. Seraphin, Solar energy conversion: solid state physics aspects, Topics in Applied Physics, vol. 31, Springer, Berlin, 1979, 24–35.

B. Carlsson, K. Möller, M. Köhl, U. Frei, S. Brunold, Qualification test procedure for solar absorber surface durability, Sol. Energy Mater. Sol. Cells 61 (2000) 255–275.

C. S. Uma, L.K. Malhotra, K.L. Chopra, Spectrally selective surfaces on stainless steel produced by chemical conversion, Thin solid films 147 (1987) 243-249.

Chao-Ching Chang, Ching-Li Huang, Cheng-Liang Chang, Poly(urethane)-based solar absorber coatings containing nano gold, Solar Energy 91 (2013) 350–357.

D.L. Douglass, R.B. Pettit, The selective solar absorptance of in situ-grown oxide films on metals, Solar Energy Materials 4 (1981) 383-402.

Duffie, J. A., Beckman, W.A., 1991. Solar Engineering of Thermal Processes. Wiley-Interscience, New York.

D. Tulchinsky , V. Uvarovb, I. Popov , D. Mandler, S. Magdassi, A novel non-selective coating material for solar thermal potential application formed by reaction between sol–gel titania and copper manganese spinel, Solar Energy Materials and Solar Cells 120 (2014) 23 – 29.

D. Tulchinsky, V. Uvarov, I. Popov , D. Mandler, S. Magdassi, A novel non-selective coating material for solar thermal potential application formed by reaction between sol–gel titania and copper manganese spinel, Solar Energy Materials & Solar Cells 120 (2014) 23–29.

Ewa Wackelgard*, Characterization of black nickel solar absorber coatings electro plated in a nickel chlorine aqueous solution, Solar Energy Materials & Solar Cells 56 (1998) 35-44.

E. Wäckelgård, G. A. Niklasson, C. G. Granqvist, Selectively solar-absorbing coatings, in: J.Gordon (Ed.), Solarenergy – The State of the Art, Firsted., James & James, London,2001,pp.109–144.(ISE Spositionpapers).

F.S. Boydag, The optical properties of some steel surfaces with different surface preparations for high temperature use, Solar Energy Materials 13 (1986) 185-195.

Gordon, J., 2001. Solar Energy, the State of the Art. James & James, London.

G. Katumba, G. Makiwa, T.R. baisitese, L. Olumekor, A. Forbes, E. Wackelgard, Solar selective absorber functionality of carbon nanoparticles embedded in SiO_2, ZnO, NiO matrices, Phys. Stat. Sol. (c) 5 (2008), 549-551.

H. Price, C. Gummo, M.J. Hale, R. Fimbres, R. Mahoney, R. Cipriani, Developments in high-temperature parabolic trough receiver technology, in:International Solar Energy Conference, Portland, OR, United States, 11–14 July.2004, article no. 65178, 2004, pp. 659–667.

H.C. Barshilia, N. Selvakumar, K.S. Rajam, A. Biswas, Structure and optical properties of pulsed sputter deposited $Cr_xO_y/Cr/Cr_2O_3$ solar selective coatings, Journal of Applied Physics 103 (2008) 1-11.

H. C. Barshilia, N. Selvakumar, K.S. Rajam, A. Biswas, Optical properties and thermal stability of TiAlN/AlON tandem absorber prepared by reactive DC/RF magnetron sputtering, Solar Energy Materials and Solar Cells 92 (2008) 1425–1433.

Hsin-Yen Cheng, Jau-Wern Chiou, Jyh-Ming Ting, Yonhua Tzeng, Reactively co-sputter deposited a-C: H/Cr thin films: Material characteristics and optical properties, Thin Solid Films 529 (2013) 164–168.

J. A. Duffie, W.A. Beckman, Solar Engineering of Thermal Processes. Wiley-Inter science, New York, 1991.

J. Vince, A.S. Vuk, U.O. Krasovec, B. Orel, M. Kohl, M.Heck, Solar absorber coatings based on CoCuMnOx spinels prepared via the sol–gel process: structural and optical properties, Solar Energy Materials and Solar Cells 79 (2003) 313–330.

K. R. Newby, Functional chromium plating, Metal Finishing 97 (1999) 223–247.

Kennedy, C.E., 2002. Review of Mid- to High-Temperature Solar Selective Absorber Materials. NREL Tech Report, NREL/TP-520-31267.

K.D. Lee, Preparation and characterization of black chrome solar selective coatings, Journal of the Korean Physical Society 51(2007) 135–144.

L. Aries, P. Fort, J.A. Flores, J.P. Traverse, Analysis of the conversion coating on Ferric stainless steel of selective absorbers, Solar Energy Materials 14 (1986) 143-159.

L. Aries, D. Fraysse, J.P. Traverse, R. Calsou, Growth of selective coating on stainless steel, Thin Solid films 151 (1987) 413-428.

L. Aries, M. El Bakkouri, J.Roy, J.P. Traverse, Thermal oxidation study of thin magnetite-based coating from iron-chromium alloys, Thin solid films 197 (1991) 143-155.

L. Wu, J. Gao, Z. Liu, L. Liang, F. Xia, H. Cao, Thermal aging characteristics of CrN_xO_y solar selective absorber coating for flat plate solar thermal collector applications, Solar Energy Materials & Solar Cells 114 (2013) 186–191.

M. Adsten, R. Joerger, K. Järrendahl, E. Wäckelgård, Optical characterization of industrially sputtered nickel-nickel oxide solar selective surface, Solar Energy 68 (2000) 325-328.

M.K. Öhl, M. Heck, S. Brunold, U. Frei, B. Carlsson, K.M. Öller, Advanced procedure for the assessment of the life time of solar absorber coatings, Sol. Energy Mater. Sol. Cells 84 (2004) 275–289.

M. Koželj, A.Š. Vuk, I. Jerman, B. Orel, Corrosion protection of Sunselect, a spectrally selective solar absorber coating, by(3-mercaptopropyl)trimethoxysilane, SolarEnergyMaterials and SolarCells 93 (2009)1733–1742.

M. Lundh, T. Blom, E. Wackelgard, Antireflection treatment of Thickness Sensitive Spectrally Selective (TSSS) paints for thermal solar absorbers, Solar Energy 84 (2010) 124–129.

Martin Joly, Yannik Antonetti, Martin Python, Marina Gonzalez, Thomas Gascou, Jean-Louis Scartezzini, Andreas Schuler, Novel black selective coating for tubular solar absorbers based on a sol–gel method, Solar Energy 94 (2013) 233–239.

Nunes, V.Teixeira, M. L. Prates, N. P. Barradas, A. D. Sequeira, Graded selective coatings based on chromium and titanium oxynitride, Thin Solid Films 442 (2003)173–178.

N. Selvakumar, H.C. Barshilia, Review of physical vapour deposited (PVD) spectrally selective coatings for mid to high-temperature solar thermal applications, Solar Energy Materials and Solar Cells 98 (2012) 1-23.

Q. C. Zhang, Stainless-Steel-AlN cermet selective surface deposited by direct current magnetron sputtering technology, Solar Energy Materials and Solar Cells 52 (1998) 95–106.

R. Juang, Y. Yeh, B. Chang, W. Chen, T. Chung, Preparation of solar selective absorbing coatings by magnetron sputtering from a single stainless steel target, Thin Solid Films 518 (2010) 5501–5504.

S. Sakthivel, V. Premkumar and A. Srinivas Rao “An improved solar selective absorber coating with excellent optical absorptance, low thermal emissivity and excellent corrosion resistance property and a process of producing the same” Indian patent Application no. 1129/DEL/2013.

S.A. Kalogirou, Solar thermal collectors and applications, Progress in Energy and Combustion Science 30 (2004) 231–295.

The method for the emissivity measurement of the heater using FTIR is prescribed in Japanese Industrial Standards JIS R 1801.

T. Bostrom, E. Wackelgard, G. Westin, Solution-chemical derived nickel–alumina coatings for thermal solar absorbers, Solar Energy 74 (2003) 497–503.

T. K. Bostrom, E. Wackelgard, G. Westin, Durability tests of solution-chemically derived spectrally selective absorbers, Solar Energy Materials and Solar Cells 89 (2005) 197–207.

T. Bostrom, J. Jensen, S. Valizadeh, G. Westin, E. Wackelgard, ERDA of Ni-Al2O3/SiO2 solar thermal selective absorber, Solar Energy materials and solar cells 92 (2008) 1177-1182.

T. N. L. Andrea Ambrosini, Chad L. Staiger, Aaron C. Hall, Marlene, Bencomo, Ellen B. Stechel, Improved High Temperature Solar Absorbers for use in Concentrating Solar Power Central Receiver Applications, Sandia National Laboratories, Albuquerque, New Mexico 87185 and Livermore, California 94550, 2010.

V. C. Sharma, A. Sharma, P. Ilenikhena, Chemical oxidation and spectral selectivity of Austenitic stainless steel AISI 321 (For use in solar-Energy Application), Energy 13 (1988) 749-754.

V. Moise, R. Cloots, A. Rulmont, Study of the electrochemical synthesis of selective black coatings absorbing solar energy, International Journal of Inorganic Materials 3 (2001) 1323–1329.

V. Teixeira, E. Sousa, M. F. Costa, C. Nunes, L. Rosa, M. J. Carvalho, M. Collares- Pereira, E. Roman, J. Gago, Spectrally selective composite coatings of Cr–Cr_2O_3 and Mo–Al_2O_3 for solar energy applications, Thin Solid Films 392 (2001) 320–326.

V. Teixeira*, E. Sousa, M.F. Costaa, C. Nunes, L. Rosa, M.J. Carvalhob, M. Collares-Pereira, E. Roman, J. Gago, Chromium-based thin sputtered composite coatings for solar thermal collectors, Vacuum 64 (2002) 299–305.

W. Graf, F. Brucker, M. Köhl, T. Tröscher, V. Wittwer, L. Herlitze, Development of large area sputtered solarabsorber coatings, Journal of Non-Crystalline Solids 218 (1997) 380–387.

Y. Yin, Y. Pan, L.X. Hang, D.R. McKenzie, M.M.M. Bilek, Direct current reactive sputtering Cr–Cr_2O_3 cermet solar selective surfaces for solar hot water applications, Thin Solid Films 517 (2009) 1601-1606.

Z. Zeng, A.Liang, J.Zhang., A review of recent patents on trivalent chromium plating, Recent Patents on Materials Science2 (2009) 50–57.